The Journal of Chemical Physics

Ehrenfest+R dynamics. II. A semiclassical QED framework for Raman scattering

Cite as: J. Chem. Phys. **150**, 044103 (2019); https://doi.org/10.1063/1.5057366
Submitted: 13 September 2018 . Accepted: 13 December 2018 . Published Online: 24 January 2019

Hsing-Ta Chen, Tao E. Li, Maxim Sukharev, Abraham Nitzan, and Joseph E. Subotnik

View Online Export Citation CrossMark

ARTICLES YOU MAY BE INTERESTED IN

Ehrenfest+R dynamics. I. A mixed quantum–classical electrodynamics simulation of spontaneous emission
The Journal of Chemical Physics **150**, 044102 (2019); https://doi.org/10.1063/1.5057365

A comparison of surface hopping approaches for capturing metal-molecule electron transfer: A broadened classical master equation versus independent electron surface hopping
The Journal of Chemical Physics **150**, 041711 (2019); https://doi.org/10.1063/1.5050235

The symmetrical quasi-classical approach to electronically nonadiabatic dynamics applied to ultrafast exciton migration processes in semiconducting polymers
The Journal of Chemical Physics **149**, 044101 (2018); https://doi.org/10.1063/1.5037815



© 2019 Author(s).

The Journal of Chemical Physics ARTICLE scitation.org/journal/jcp

Ehrenfest+R dynamics. II. A semiclassical QED framework for Raman scattering

Cite as: J. Chem. Phys. 150, 044103 (2019); doi: 10.1063/1.5057366
Submitted: 13 September 2018 • Accepted: 13 December 2018 •
Published Online: 24 January 2019

View Online Export Citation CrossMark

Hsing-Ta Chen,[1,a)] Tao E. Li,[1] Maxim Sukharev,[2,3] Abraham Nitzan,[1] and Joseph E. Subotnik[1]

AFFILIATIONS

[1] Department of Chemistry, University of Pennsylvania, Philadelphia, Pennsylvania 19104, USA
[2] Department of Physics, Arizona State University, Tempe, Arizona 85287, USA
[3] College of Integrative Sciences and Arts, Arizona State University, Mesa, Arizona 85212, USA

[a)] **Electronic mail:** hsingc@sas.upenn.edu

ABSTRACT

In Paper I [Chen *et al.*, J. Chem. Phys. **150**, 044102 (2019)], we introduced Ehrenfest+R dynamics for a two-level system and showed how spontaneous emission can be heuristically included such that, after averaging over an ensemble of Ehrenfest+R trajectories, one can recover both coherent and incoherent electromagnetic fields. In the present paper, we now show that Ehrenfest+R dynamics can also correctly describe Raman scattering, whose features are completely absent from standard Ehrenfest dynamics. Ehrenfest+R dynamics appear to be quantitatively accurate both for resonant and off-resonant Raman signals, as compared with Kramers–Heisenberg–Dirac theory.

Published under license by AIP Publishing. https://doi.org/10.1063/1.5057366

I. INTRODUCTION

Recently there has been an explosion of interest in Raman scattering, especially surface- and tip-enhanced Raman scattering,[1–6] as a probe to investigate plasmonic excitations of molecules near a metal surface[7–10] and chemical reactions at catalytic surfaces.[11] In general, the Raman technique offers an experimentalist detailed information about how molecular vibrations couple to charges through electronic polarization,[12,13] and the Raman technique is very relevant for modern experiments with metallic nanoclusters.[14] Raman spectroscopy can also often provide clean signals for characterizing biological materials in an aqueous medium (with otherwise complex IR absorption spectra).[15]

From a quantitative point of view, the current theory of molecular Raman scattering is based on the Kramers–Heisenberg–Dirac (KHD) formalism[16,17] which can be reduced to Placzek's classical theory of polarizability for off resonance cases,[18,19] as well as Albrecht's vibronic theory for resonant Raman scattering.[20–22] Over the years, efficient semiclassical tools have been developed to evaluate Raman spectra approximately within the KHD formalism using an excited-state gradient approximation to propagate short time dynamics.[19,23–26] More recently, chemists have also incorporated electronic structure theories into the semiclassical description of Raman spectroscopy[27–30] based on the time-dependent picture developed by Heller *et al.*[24,25] In general, because it relies on a sum over all states (nuclear and electronic), the KHD formalism can be difficult to implement in practice.

One long term goal for our research effort is to study plasmonic systems under strong light–matter coupling conditions where Raman scattering is a very sensitive probe of the collective behavior of electronic dynamics.[31,32] For such systems, a direct implementation of KHD theory is not feasible (because of the large number of states required) and is also likely not relevant (because strong coupling conditions should invalidate perturbation theory). Thus, in order for us to model such systems, and to take into account strong light–matter couplings, the most natural approach is to consider the quantum subsystems and classical electromagnetic (EM) fields on an equal footing. This approach stands in contrast

Published under license by AIP Publishing

to most existing semiclassical approaches for spectroscopy, which treat the incoming field as a fixed external perturbation and extrapolate the behavior of quantum subsystems to predict light emission.[23,24,33,34]

Now, obviously, any computational approach to spectroscopy that promises "equal footing" for light and matter will necessarily require drastic approximations; in particular, we expect that a quantum treatment of the EM field will be prohibitively difficult, and one will necessarily need to work with classical EM fields.[35] The simplest example of such a mixed quantum–classical approach is self-consistent Ehrenfest dynamics. Unfortunately, Ehrenfest dynamics does not fully recover spontaneous emission and thus is unlikely to capture Raman scattering either.[35,36] That being said, we are unaware of a systematic study addressing this question.

In Paper I, we proposed an improved so-called "Ehrenfest+R" algorithm that builds in spontaneous emission on top of Ehrenfest dynamics by enforcing additional relaxation for two-level systems.[37] In this paper, our goal is to generalize Ehrenfest+R to the case of a multi-level quantum subsystem. We will show that such a generalization can capture both resonant and off-resonant Raman scattering (at least for a three-level molecular system). Our results are in quantitative agreement with KHD theory. The data presented here strongly suggest that Ehrenfest+R dynamics (and other spruced-up versions of mean-field dynamics) can be excellent tools for exploring interesting light–matter interactions far beyond simple linear absorption or Raman phenomena (and also applicable to large subsystems, e.g., exciton–plasmon systems).

This article is organized as follows. In Sec. II, we review the KHD formalism and calculate the polarizability and Raman scattering profile for a three-level system. In Sec. III, we formulate an Ehrenfest+R approach for a three-level system. In Sec. IV, we show Ehrenfest+R dynamics results for Raman spectra and compare against the KHD formalism. In Sec. V, we conclude with an outlook for the future. In this article, we use a bold symbol to denote a space vector in the Cartesian coordinate, such as $\mathbf{E}(\mathbf{r}) = E_x(\mathbf{r})\hat{\mathbf{x}} + E_y(\mathbf{r})\hat{\mathbf{y}} + E_z(\mathbf{r})\hat{\mathbf{z}}$, and $\widehat{H}$ denotes a quantum operator. We work in SI units.

II. QUANTUM THEORY OF RAMAN SCATTERING

Raman light scattering is an inelastic process whereby the interaction between the incident photons and molecules can lead to an energy shift in emission spectra for a small fraction of the scattered photons. To qualitatively describe Raman light scattering, consider a molecular system with interactions between electronic states and nuclear vibrations. Incident photons excite the molecular system to an intermediate state (which could be a virtual state), and that intermediate state is subsequently coupled both to the ground state and to other vibronic states. Thus, the system can emit photons with two different frequencies through spontaneous emission.[38] On the one hand, a transition back to the ground state yields scattered photons with the same energy with the incident photons (which is known as Rayleigh scattering). On the other hand, a transition to other vibronic states will generate scattered photons with energies different from the incident photons (which is known as Raman scattering).

In this section, we review the KHD dispersion formula which quantifies the Raman scattering cross section,[16,17,20] assuming the knowledge of the polarizability and we evaluate the KHD formalism for a three-level model system in 1D space.

A. Kramers–Heisenberg–Dirac formalism

For a quantitative description of Raman scattering, the KHD formula is the standard, frequency domain expression for the scattering cross section[19]

$$\sigma_{\hat{f}\hat{i}}^{\mathrm{3D}}(\omega_S,\omega_I) = \frac{8\pi\omega_I\omega_S^3}{9c^4}\sum_{\rho,\lambda}\left|\left[\alpha_{\hat{f}\hat{i}}(\omega_I)\right]^{\nu\nu'}\right|^2, \tag{1}$$

where the polarizability is given by

$$\left[\alpha_{\hat{f}\hat{i}}(\omega_I)\right]^{\nu\nu'} = -\sum_{k,n}\left(\frac{\left\langle\psi_f\middle|\widehat{\mu}^{\nu}\middle|\psi_{k,n}\right\rangle\left\langle\psi_{k,n}\middle|\widehat{\mu}^{\nu'}\middle|\psi_i\right\rangle}{\varepsilon_i+\hbar\omega_I-\varepsilon_{kn}+i\hbar\gamma} + \frac{\left\langle\psi_f\middle|\widehat{\mu}^{\nu'}\middle|\psi_{k,n}\right\rangle\left\langle\psi_n\middle|\widehat{\mu}^{\nu}\middle|\psi_i\right\rangle}{\varepsilon_f-\hbar\omega_I-\varepsilon_{kn}+i\hbar\gamma}\right). \tag{2}$$

The frequency of the incident photons is ω_I, and the frequency of the scattered photons is ω_S; these frequencies satisfy energy conservation $\hbar\omega_S = \varepsilon_i + \hbar\omega_I - \varepsilon_f$. The KHD formula is known as the "sum-over-states" formula since the polarizability expression requires a summation over all possible intermediate states $\psi_{k,n}$, where the index k labels electronic states and the index n labels vibrational states corresponding to electronic states. $\widehat{\mu}^{\nu}$ denotes the transition dipole moment operator for $\nu = \{x,y,z\}$. The linewidth γ corresponds to the average lifetime of the intermediate state.[28,29]

According to the scattering cross section given by Eq. (1), Raman spectroscopy is a two-photon spectroscopy. Experimentally, one typically fixes ω_I and observes the emission spectrum as a function of ω_S. The frequency $\omega_S = \omega_I$ corresponds to the contribution of Rayleigh scattering, and other emission peaks are attributed to Raman scattering. The KHD formula is derived using second order perturbation theory for a quantum subsystem in the presence of the incident photons,[19] and the scattering cross section is extrapolated from the change in electronic population.

B. Three-level system

To quantify the KHD Raman scattering formalism, we consider a three-level system ($|0\rangle$, $|1\rangle$, $|2\rangle$) with the energies $\varepsilon_0 \le \varepsilon_1 < \varepsilon_2$. We assume that the electric dipole interactions couple the states $0 \leftrightarrow 2$ and $1 \leftrightarrow 2$ only (i.e., a Λ-type coupling system). Thus, the electronic Hamiltonian is time-dependent

Published under license by AIP Publishing

and given by

$$\hat{H}^{el}(t) = \begin{pmatrix} \varepsilon_0 & 0 & \mathcal{V}_{02}(t) \\ 0 & \varepsilon_1 & \mathcal{V}_{12}(t) \\ \mathcal{V}_{02}^*(t) & \mathcal{V}_{12}^*(t) & \varepsilon_2 \end{pmatrix}, \tag{3}$$

where the electric dipole coupling is

$$\mathcal{V}_{ij}(t) = -\int dx \mathbf{E}(x,t) \cdot \mathcal{P}_{ij}(x). \tag{4}$$

Here we are working in 1D.

For frequency domain measurements, consider a single-mode incoming continuous wave (CW) electromagnetic field with frequency ω_I,

$$\mathbf{E}_I(x,t) = \frac{A_I}{\sqrt{\epsilon_0}} \cos(k_I x - \omega_I t)\hat{\mathbf{z}}, \tag{5}$$

$$\mathbf{B}_I(x,t) = -\sqrt{\mu_0} A_I \sin(k_I x - \omega_I t)\hat{\mathbf{y}}, \tag{6}$$

where $\omega_I = ck_I$ and A_I is the amplitude of the incoming field. We assume that the spatial size of the polarization is small in space, i.e., $\mathcal{P}_{ij}(x) \approx \mu_{ij}\delta(x)\hat{\mathbf{z}}$, so that the electric dipole interactions are approximated as $\int dx \mathbf{E}(x,t) \cdot \mathcal{P}_{ij}(x) \approx \mu_{ij} \frac{A_I}{\sqrt{\epsilon_0}} \cos(\omega_I t)$.

For light scattering in a 1D space, the scattering cross section is defined as the ratio between the number of photons scattered per time divided by the number of incident photons per time. With this definition, the KHD Raman cross section becomes in 1D (see Appendix A)

$$\sigma_{fi}^{1D}(\omega_S, \omega_I) = \frac{\omega_I \omega_S}{2c^2} \left| \alpha_{fi}^{1D}(\omega_I) \right|^2. \tag{7}$$

For a three-level system, the KHD expression for the polarizability for $i, f = 0, 1$ is

$$\alpha_{10}^{1D}(\omega_I) = -\left(\frac{\mu_{02}\mu_{12}}{\varepsilon_0 + \hbar\omega_I - \varepsilon_2 + i\hbar\gamma} + \frac{\mu_{02}\mu_{12}}{\varepsilon_1 - \hbar\omega_I - \varepsilon_2 + i\hbar\gamma} \right). \tag{8}$$

Analogous expression holds for α_{01}; note that $\alpha_{10} \neq \alpha_{01}$. Here we take linewidth γ to be the lifetime for the electronic transitions of the excited state

$$\frac{1}{\gamma} = \frac{1}{2}\left(\frac{1}{\kappa_{02}} + \frac{1}{\kappa_{12}} \right), \tag{9}$$

where the corresponding Fermi's golden rule (FGR) rates are given by

$$\kappa_{fi} = \frac{\varepsilon_i - \varepsilon_f}{\hbar^2 \epsilon_0 c} \mu_{fi}^2. \tag{10}$$

In the case of resonant Raman scattering (where the incident photon lines up with the excited state, i.e., $\varepsilon_i + \hbar\omega_I = \varepsilon_2$), the first term in Eq. (8) dominates. Resonant Raman scattering signals are composed of two signals: (i) When $\hbar\omega_I = \varepsilon_2 - \varepsilon_0$ and the scattered photon energy is $\hbar\omega_S = \varepsilon_2 - \varepsilon_1$, the polarizability term with $i = 0$ and $f = 1$ ($\alpha_{10}^{1D}(\omega_I)$) leads to a Stokes Raman peak (i.e., $\omega_S < \omega_I$). (ii) When $\hbar\omega_I = \varepsilon_2 - \varepsilon_1$, the scattered photon energy is $\hbar\omega_S = \varepsilon_2 - \varepsilon_0$, and the analogous polarizability term with $i = 1$ and $f = 0$ ($\alpha_{01}^{1D}(\omega_I)$) leads to an anti-Stokes Raman peak (i.e., $\omega_S > \omega_I$). Obviously, anti-Stokes Raman scattering can occur only if state $|1\rangle$ is occupied at steady state.

In the case that the incident photon does not line up with any excited state, the excitation is detuned far off resonance (known as off-resonance Raman scattering). In this off-resonant case, the intermediate state of the light scattering process is a virtual state, i.e., $\varepsilon_k = \varepsilon_i + \hbar\omega_I$, and the two terms in Eq. (8) both contribute meaningfully to the Raman cross section. Of course, for a weak field, scattered photons are always dominated by Rayleigh scattering (i.e., $\omega_S = \omega_I$). Note that, in the absence of pure dephasing, there should not be any fluorescence observed in the scattered field.[38]

III. EHRENFEST+R APPROACH FOR RAMAN SCATTERING

Given that Raman scattering is based on spontaneous emission,[38] Ehrenfest+R dynamics should provide a proper tool for a mixed quantum-classical simulation since the algorithm was designed to recover spontaneous emission. One can generalize the Ehrenfest+R method to the case of more than a two-level system as follows: we add distinct +R corrections for electronic transitions between individual pairs of states, i.e., $2 \rightarrow 0$ and $2 \rightarrow 1$. (And this approach can clearly be applied to treat even more quantum states as well.) Furthermore, to reach the steady state, we allow a phenomenological, non-radiative dissipation between $|0\rangle$ and $|1\rangle$. In this section, we start by formulating such a generalized Ehrenfest+R approach in the context of a three-level system; thereafter, we compare Ehrenfest+R results against the KHD formula.

A. Generalized Ehrenfest+R method

For the Hamiltonian given by Eq. (3), there are two electronic transitions that are mediated by electric dipole couplings $\mathcal{V}_{02}$ and $\mathcal{V}_{12}$ corresponding to spontaneous emission rates κ_{02} and κ_{12} given by Eq. (10). Here, based on Ref. 37, we will add two pairwise +R corrections on top of Ehrenfest dynamics in order to recover the individual spontaneous emission rates (κ_{fi}) from $|i\rangle$ to $|f\rangle$ while keeping the other state populations fixed.

1. System propagator

To implement a pairwise treatment for Ehrenfest+R dynamics, the Liouville equation (together with additional relaxations) can be written as

$$\frac{\partial \hat{\rho}}{\partial t} = -\frac{i}{\hbar}\left[\hat{H}^{el}, \hat{\rho}\right] + \hat{\hat{\mathcal{L}}}_R^{2\rightarrow 0}\hat{\rho} + \hat{\hat{\mathcal{L}}}_R^{2\rightarrow 1}\hat{\rho}. \tag{11}$$

Here, the diagonal elements of the $\hat{\hat{\mathcal{L}}}_R^{i\rightarrow f}$ super-operators are defined by

$$\left[\hat{\hat{\mathcal{L}}}_R^{i\rightarrow f}\hat{\rho}\right]_{ii} = -\left[\hat{\hat{\mathcal{L}}}_R^{i\rightarrow f}\hat{\rho}\right]_{ff} = -k_R^{fi}\rho_{ii}, \tag{12}$$

and the off diagonal element of $[\mathcal{L}_R\hat{\rho}]_{ij}$ is chosen to be

Published under license by AIP Publishing

$$\left[\widehat{\widehat{\mathcal{L}}}_{\mathrm{R}}^{i\to f}\,\widehat{\rho}\right]_{if} = \left[\widehat{\widehat{\mathcal{L}}}_{\mathrm{R}}^{i\to f}\,\widehat{\rho}\right]_{fi}^{*} = -\gamma_{\mathrm{R}}^{fi}\rho_{if}. \tag{13}$$

The +R relaxation rate k_{R}^{fi} for the transition $i \to f$ is given by

$$k_{\mathrm{R}}^{fi} \equiv 2\kappa_{fi}\left(1-\rho_{ff}\right)\mathrm{Im}\left[\frac{\rho_{fi}}{|\rho_{fi}|}e^{i\phi}\right]^{2}. \tag{14}$$

Here, the κ_{fi} is the FGR in Eq (10). $\phi \in (0, 2\pi)$ is a phase chosen randomly for each Ehrenfest+R trajectory. The +R dephasing rate γ_{R}^{fi} in Eq. (13) is chosen to be

$$\gamma_{\mathrm{R}}^{fi} \equiv \frac{\kappa_{fi}}{2}\left(1-\rho_{ff}+\rho_{ii}\right). \tag{15}$$

In practice, we use a pure state representation for the density matrix $\widehat{\rho} = |\psi\rangle\langle\psi|$, with wavefunction $|\psi(t)\rangle = c_0(t)|0\rangle + c_1(t)|1\rangle + c_2(t)|2\rangle$. The additional relaxation embodied by $\widehat{\widehat{\mathcal{L}}}_{\mathrm{R}}^{i\to f}$ is defined by a transition operator[37]

$$\widehat{\mathcal{T}}\left[k_{\mathrm{R}}^{fi}\right]\begin{pmatrix}\vdots\\ c_i\\ \vdots\\ c_f\\ \vdots\end{pmatrix} = \begin{pmatrix}\vdots\\ \frac{c_i}{|c_i|}\sqrt{|c_i|^2 - k_{\mathrm{R}}^{fi}|c_i|^2 dt}\\ \vdots\\ \frac{c_f}{|c_f|}\sqrt{|c_f|^2 + k_{\mathrm{R}}^{fi}|c_f|^2 dt}\\ \vdots\end{pmatrix}, \tag{16}$$

with a fixed relative phase between c_i and c_f, plus a stochastic random phase operator

$$e^{i\widehat{\Phi}\left[\gamma_{\mathrm{R}}^{fi}\right]}\begin{pmatrix}\vdots\\ c_i\\ \vdots\\ c_f\\ \vdots\end{pmatrix} = \begin{pmatrix}\vdots\\ e^{i\Phi_i}c_i\\ \vdots\\ e^{i\Phi_f}c_f\\ \vdots\end{pmatrix} \text{ if } \mathrm{RN} < \gamma_{\mathrm{R}}^{fi}dt. \tag{17}$$

Here RN $\in [0,1]$ is a random number, and we choose $\Phi_i = 0$, $\Phi_f \in (0, 2\pi)$ as random phases. In other words, we choose to assign a random phase only to the final state (f) which has a lower energy than the initial state (i). This choice is crucial for ensuring that, e.g., spontaneous emission from $2 \to 1$ does not affect the coherence between states 2 and 0.

Thus in practice, the time evolution of the subsystem wavefunction is carried out as

$$|\psi(t+dt)\rangle = e^{i\widehat{\Phi}\left[\gamma_{\mathrm{R}}^{12}\right]}\widehat{\mathcal{T}}\left[k_{\mathrm{R}}^{12}\right] \times e^{i\widehat{\Phi}\left[\gamma_{\mathrm{R}}^{02}\right]}\widehat{\mathcal{T}}\left[k_{\mathrm{R}}^{02}\right]e^{-i\widehat{\mathrm{H}}^{\mathrm{el}}dt/\hbar}|\psi(t)\rangle, \tag{18}$$

where $e^{-i\widehat{\mathrm{H}}^{\mathrm{el}}dt/\hbar}$ is responsible for propagating according to the first term of Eq. (11). Note that $e^{i\widehat{\Phi}\left[\gamma_{\mathrm{R}}^{12}\right]}\widehat{\mathcal{T}}\left[k_{\mathrm{R}}^{12}\right]$ and $e^{i\widehat{\Phi}\left[\gamma_{\mathrm{R}}^{02}\right]}\widehat{\mathcal{T}}\left[k_{\mathrm{R}}^{02}\right]$ commute as long as dt is sufficiently small.

2. EM field propagator

We write the total EM field in the form of $\mathbf{E} = \mathbf{E}_{\mathrm{I}} + \mathbf{E}_{\mathrm{S}}$ and $\mathbf{B} = \mathbf{B}_{\mathrm{I}} + \mathbf{B}_{\mathrm{S}}$, where $\mathbf{E}_{\mathrm{S}}$ and $\mathbf{B}_{\mathrm{S}}$ are the scattered EM fields. For a CW field given by Eqs. (5) and (6), $\mathbf{E}_I$ and $\mathbf{B}_{\mathrm{I}}$ satisfy source-less Maxwell's equations, so we can treat the CW field as a standalone external field. Therefore, for the underlying Ehrenfest dynamics, the scattered fields $\mathbf{E}_{\mathrm{S}}$ and $\mathbf{B}_{\mathrm{S}}$ satisfy Maxwell's equations

$$\frac{\partial}{\partial t}\mathbf{B}_{\mathrm{S}} = -\boldsymbol{\nabla}\times\mathbf{E}_{\mathrm{S}}, \tag{19}$$

$$\frac{\partial}{\partial t}\mathbf{E}_{\mathrm{S}} = c^2\boldsymbol{\nabla}\times\mathbf{B}_{\mathrm{S}} - \frac{1}{\epsilon_0}\mathbf{J}, \tag{20}$$

where the average current is

$$\mathbf{J}(x,t) = \sum_{i=2}\sum_{f=0,1} 2\left(\varepsilon_f - \varepsilon_i\right)\mathrm{Im}\left[\rho_{fi}(t)\right]\mathcal{P}_{fi}(x). \tag{21}$$

Given the pairwise transitions of the subsystem, the classical EM field must be rescaled. We denote the rescaling operator for the EM fields by

$$\mathcal{R}\left[\delta U_{\mathrm{R}}^{fi}\right]:\begin{pmatrix}\mathbf{E}_{\mathrm{S}}\\ \mathbf{B}_{\mathrm{S}}\end{pmatrix}\to\begin{pmatrix}\mathbf{E}_{\mathrm{S}}+\eta^{fi}\delta\mathbf{E}_{\mathrm{R}}^{fi}\\ \mathbf{B}_{\mathrm{S}}+\xi^{fi}\delta\mathbf{B}_{\mathrm{R}}^{fi}\end{pmatrix}, \tag{22}$$

where the rescaling coefficients are chosen to be

$$\eta^{fi} = \sqrt{\frac{cdt}{\Lambda^{fi}}\frac{\delta U_{\mathrm{R}}^{fi}}{\epsilon_0\int dv\left|\delta\mathbf{E}_{\mathrm{R}}^{fi}\right|^2}}\times\mathrm{sgn}\left(\mathrm{Im}\left[\rho_{fi}e^{i\phi}\right]\right), \tag{23}$$

$$\xi^{fi} = \sqrt{\frac{cdt}{\Lambda^{fi}}\frac{\mu_0\delta U_{\mathrm{R}}^{fi}}{\int dv\left|\delta\mathbf{B}_{\mathrm{R}}^{fi}\right|^2}}\times\mathrm{sgn}\left(\mathrm{Im}\left[\rho_{fi}e^{i\phi}\right]\right). \tag{24}$$

Here Λ^{fi} is the self-interference length (see Ref. 37). For a Gaussian polarization profile [as in Eq. (33)], $\Lambda^{fi} = 2.363/\sqrt{2a}$. The energy change for each pairwise relaxation $i \to f$ is

$$\delta U_{\mathrm{R}}^{fi} = \left(\varepsilon_i - \varepsilon_f\right)k_{\mathrm{R}}^{fi}\rho_{ii}dt. \tag{25}$$

According to Eq. (18), we need to apply two rescaling operators ($\mathcal{R}\left[\delta U_{\mathrm{R}}^{12}\right]$ and $\mathcal{R}\left[\delta U_{\mathrm{R}}^{02}\right]$) corresponding to the two relaxation pathways ($2 \to 0$ and $2 \to 1$).

For the results below, we assume that the transition dipole moments are the same for both the $2 \to 1$ and $2 \to 0$ transitions, i.e., $\mathcal{P}_{02} = \mathcal{P}_{12} = \mathcal{P}$, so that the rescaling fields can be chosen to be $\delta\mathbf{E}_{\mathrm{R}}^{fi} = \delta\mathbf{E}_{\mathrm{R}}$ and $\delta\mathbf{B}_{\mathrm{R}}^{fi} = \delta\mathbf{B}_{\mathrm{R}}$. For a 1D system, the rescaling fields take the form

$$\delta\mathbf{E}_{\mathrm{R}} = \boldsymbol{\nabla}\times\boldsymbol{\nabla}\times\mathcal{P} - g\mathcal{P}, \tag{26}$$

$$\delta\mathbf{B}_{\mathrm{R}} = -\boldsymbol{\nabla}\times\mathcal{P} - h(\boldsymbol{\nabla}\times)^3\mathcal{P}. \tag{27}$$

As demonstrated in Ref. 37, for the Gaussian polarization defined in Eq. (33), we choose $g = 2a$ and $h = 1/6a$. With this

Published under license by AIP Publishing

assumption, we can combine the two rescaling operators as $\mathcal{R}\left[\delta U_R^{12} + \delta U_R^{02}\right]$.

In the end, each Ehrenfest+R trajectory for classical EM fields is propagated by

$$\begin{pmatrix}\mathbf{E}_S(t+dt)\\ \mathbf{B}_S(t+dt)\end{pmatrix} = \mathcal{R}\left[\delta U_R^{12} + \delta U_R^{02}\right]\mathcal{M}[dt]\begin{pmatrix}\mathbf{E}_S(t)\\ \mathbf{B}_S(t)\end{pmatrix}. \tag{28}$$

Here $\mathcal{M}[dt]$ denotes the linear propagator of Maxwell's equations [Eqs. (19) and (20)] for time step dt.

3. Non-radiative dissipation

Without any non-radiative dissipation, the three-level system in Eq. (3) eventually reaches the asymptotic state $|\psi(t\to\infty)\rangle = |1\rangle$ in the presence of the CW field. By contrast, to reach the correct steady state, we must take into account non-radiative relaxation. Thus, we also introduce a phenomenological, non-radiative relaxation from $|1\rangle$ to $|0\rangle$ by a transition operator

$$|\psi(t+dt)\rangle \to \widehat{\mathcal{T}}\left[k_{nr}^{01}\right]|\psi(t+dt)\rangle, \tag{29}$$

where the operation of the transition operator $\mathcal{T}$ is defined in Eq. (16). The classical EM field is not rescaled for this non-radiative transition, and the non-radiative decay rate k_{nr}^{01} is an empirical parameter which will be specified later. Note that we exclude thermal transitions from $|0\rangle$ to $|1\rangle$ since we assume that the system is at a very low temperature.

In the end, Ehrenfest+R dynamics are specified by Eqs. (18), (28), and (29).

4. Coherent and incoherent emission

Our primary interest is in the scattering EM field when the system reaches the steady state ($t \to t_{ss}$) in the presence of an external CW field. Let $\left\{\mathbf{E}_S^\ell(x, t_{ss}); \ell \in N_{traj}\right\}$ be the set of scattering electric fields at a steady state for an ensemble of Ehrenfest+R trajectories (labeled by ℓ). The average electric field $\langle\mathbf{E}_S(x, t_{ss})\rangle$ represents coherent emission, and the Fourier transform of the average electric field yields the scattering spectrum for coherent emission,

$$\langle\mathbf{E}_S(\omega_S)\rangle = \int dx e^{i\omega_S x/c}\frac{1}{N_{traj}}\sum_\ell^{N_{traj}}\mathbf{E}_S^\ell(x, t_{ss}). \tag{30}$$

We expect that, in Eq. (30), all incoherent contributions with random phases will vanish when we take ensemble average. We denote the magnitude of the coherent emission intensity at scattering frequency ω_S as $|\langle\mathbf{E}_S(\omega_S)\rangle|^2$.

We now turn to the incoherent emission. The expectation value of the intensity distribution $\left\langle|\mathbf{E}_S(x, t_{ss})|^2\right\rangle$ corresponds to the energy distribution of the scattering EM field. We can obtain the total emission power spectrum by averaging over the intensity in Fourier space,

$$\left\langle|\mathbf{E}_S(\omega_S)|^2\right\rangle = \frac{1}{N_{traj}}\sum_\ell^{N_{traj}}\left|\int dx e^{i\omega_S x/c}\mathbf{E}_S^\ell(x, t_{ss})\right|^2. \tag{31}$$

Note that the total intensity in Eq. (31) includes the contributions of both coherent and incoherent scattering signals. Thus, $\left\langle|\mathbf{E}_S(\omega_S)|^2\right\rangle$ can be considered as the energy distribution of scattering photons with mode ω_S. Finally we can extract a scattering cross section from Ehrenfest+R dynamics by the formula

$$\sigma_{10}^{1D}(\omega_S, \omega_I) = \frac{\left\langle|\mathbf{E}_S(\omega_S)|^2\right\rangle/\omega_S}{A_I^2/\omega_I}, \tag{32}$$

according to the definition of the 1D scattering cross section and the Einstein relation [see Eq. (A5)].

Before concluding this section, let us once more emphasize the conclusion of Ref. 37. Within Ehrenfest+R dynamics, standard Ehrenfest dynamics yields only coherent emission; at the same time, however, the +R relaxation pathway is able to produce incoherent emission.

IV. RESULTS

As far as simulating Raman scattering by the Ehrenfest+R approach, we consider a three-level system with $\varepsilon_0 = 0$, $\varepsilon_1 = 4.115$ eV, and $\varepsilon_2 = 16.46$ eV so that we can define the frequencies of the system: $\hbar\Omega_{20} = \varepsilon_2 - \varepsilon_0$ and $\hbar\Omega_{21} = \varepsilon_2 - \varepsilon_1$. In all that follows, we will normalize all frequencies in units of $\Omega \equiv \Omega_{20} = 16.46$ eV. For instance, $\Omega_{21} = 12.345$ eV $= \frac{3}{4}\Omega$. Note that, for demonstration purposes only, we have chosen the energy scale ratio to be Ω_{20}:Ω_{21} = 1:3/4 so that we can easily observe a clear separation between the Raman peak and the Rayleigh peak in a reasonably short time. Thus, the present model is for electronic Raman scattering, rather than vibrational Raman scattering. That being said, the performance of the proposed Ehrenfest+R dynamics for Raman scattering will not depend on the particular energy difference of the three level model system and our results will be applicable to a broader regime of parameters (vibrational or electronic).

We assume that the initial state of the system is the ground state, $|\psi(t=0)\rangle = |0\rangle$, and we turn on the incident CW field at $t = 0$. The transition dipole moment takes the form of a Gaussian distribution

$$\mathcal{P}_{02}(x) = \mathcal{P}_{12}(x) = \mu\sqrt{\frac{a}{\pi}}e^{-ax^2}\hat{\mathbf{z}}, \tag{33}$$

where $\mu = 11\,282$ C/(nm/mol) and $a = 1/2\sigma^2$ with $\sigma = 3.0$ nm. With this polarization, the rescaling fields are (from Ref. 37)

$$\delta\mathbf{E}_R(x) = -\mu\sqrt{\frac{a}{\pi}}4a^2x^2e^{-ax^2}\hat{\mathbf{z}}, \tag{34}$$

$$\delta\mathbf{B}_R(x) = \mu\sqrt{\frac{a}{\pi}}\frac{4}{3}a^2x^3e^{-ax^2}\hat{\mathbf{y}}. \tag{35}$$

The average lifetime is $1/\gamma \approx 40$ fs. We run dynamics for $t_{ss} = 200$ fs to reach a steady state, averaging over $N_{traj} = 400$ trajectories. For the non-radiative dissipation, we choose a non-radiative decay rate to be $k_{nr}^{01}/\gamma = 37.33$. Note that, as long

Published under license by AIP Publishing

as $k_{nr}^{01} \gg \gamma$ is large enough, our results do not depend on the choice of k_{nr}^{01}.

A. Resonance and off resonance scattering

We first focus on Raman scattering in the frequency-domain spectrum. In Fig. 1, we plot the spectrum of coherent emission and total scattering at the steady state as a function of ω_S for various incident frequencies ω_I. In Fig. 1(a), we plot results from Ehrenfest dynamics, and in Fig. 1(b), we plot results from Ehrenfest+R dynamics. When the incident field is far from resonance, we find that the scattered EM field is dominated by Rayleigh scattering ($\omega_S = \omega_I$), as expected from the KHD formula. Qualitatively, both standard Ehrenfest dynamics and Ehrenfest+R dynamics predict Rayleigh scattering peaks at the correct frequency and show a linear shift with respect to the incident frequency. When the incident photon is at resonance (i.e., the incident frequency ω_I lines up with electronic excitation), Ehrenfest+R dynamics captures Raman scattering peaks at $(\omega_I, \omega_S) = (\Omega_{20}, \Omega_{21})$. Note that anti-Stokes Raman scattering is relatively weak here.

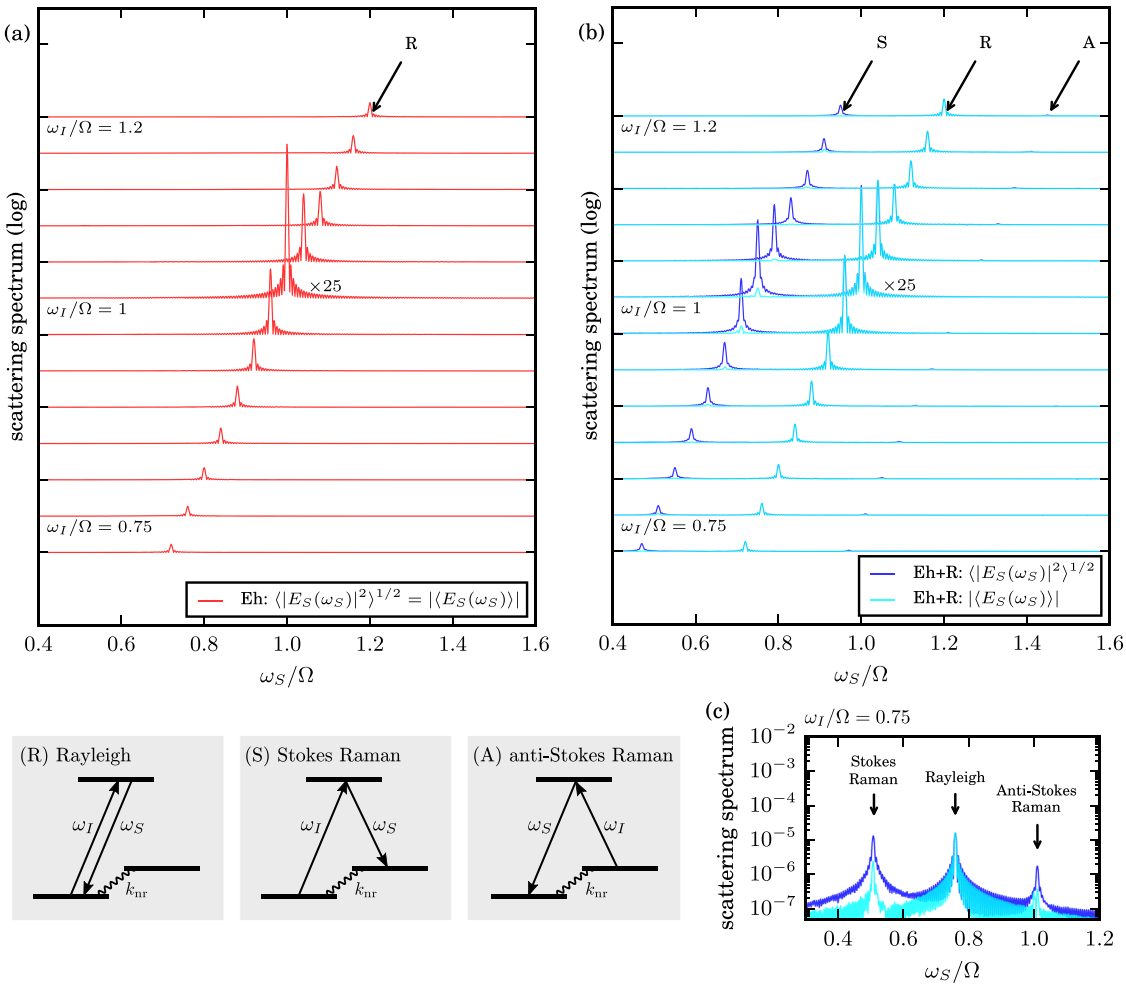


FIG. 1. Raman scattering spectra as a function of ω_S/Ω when varying the incident CW field frequency ω_I/Ω. We plot the total intensity spectrum $\left\langle|\mathbf{E}_S(\omega_S)|^2\right\rangle^{1/2} = |\langle\mathbf{E}_S(\omega_S)\rangle|$ obtained by standard Ehrenfest dynamics in (a). For Ehrenfest+R dynamics, we plot both the coherent emission spectrum $|\langle\mathbf{E}_S(\omega_S)\rangle|$ (colored cyan) and the total intensity spectrum $\left\langle|\mathbf{E}_S(\omega_S)|^2\right\rangle^{1/2}$ (colored blue). The incoming field amplitude is $A_I/\sqrt{\hbar\Omega} = 6 \times 10^{-3}$. For all CW frequencies, Rayleigh scattering peaks are observed at $\omega_S = \omega_I$. Stokes Raman scattering is always observed at $\omega_S = \omega_I - \frac{1}{4}\Omega$. In the case of resonant Raman, when $\omega_I/\Omega = 1$, a strong Stokes signal occurs at $\omega_S/\Omega = \frac{3}{4}$; there is also a small anti-Stokes signal occurring at $\omega_S/\Omega = 1$ when $\omega_I/\Omega = \frac{3}{4}$. Obviously, the anti-Stokes resonant Raman signal is always much smaller than the Stokes Raman signal, on or off resonance. (c) A semi-log plot of the scattering spectrum for $\omega_I/\Omega = \frac{3}{4}$. With this log scale, one can clearly see that Ehrenfest+R dynamics recovers both Stokes and anti-Stokes Raman scattering peaks (whereas standard Ehrenfest dynamics produces only Rayleigh scattering). Note also that only Rayleigh scattering comes in the form of a coherent emission field; Raman scattering are both incoherent emission fields.

Published under license by AIP Publishing

In contrast to Ehrenfest+R dynamics, we also plot the spectra obtained from standard Ehrenfest calculations in Fig. 1(a). From Fig. 1, we must emphasize that Ehrenfest dynamics capture only Rayleigh scattering peaks, but not Raman scattering peaks. To rationalize this behavior, we recall that the Ehrenfest decay rate for spontaneous emission depends linearly on the lower state population.[37] For the initial state $c_0 = 1$ and $c_1 = c_2 = 0$, the system is excited to state $|2\rangle$ by the incident field, but will never populate state $|1\rangle$. Therefore, effectively we always have $c_1 = 0$ within Ehrenfest dynamics and the spontaneous emission via electronic transition $2 \rightarrow 1$ never occurs. As a general rule of thumb, because standard Ehrenfest dynamics are effectively classical dynamics, whereas there is only a single frequency ω_I in the EM field and the EM field strength is weak, Ehrenfest dynamics will predict all responses to be at the same frequency ω_I.

B. Coherent emission and total intensity

Several words are now appropriate regarding the character of the outgoing fields: are they coherent (with $|\langle \mathbf{E}_S \rangle|^2 = \langle |\mathbf{E}_S|^2 \rangle$), are they partially coherent, or are they totally incoherent? In Fig. 1(b), we observe that Rayleigh scattering is made up of completely coherent emission according to Ehrenfest+R dynamics. For an elastic scattering process ($\omega_S = \omega_I$) such as Rayleigh scattering, the outgoing field retains the phase of the incoming field so that the signal is not canceled out in the average electric field $\langle \mathbf{E}_S(\omega_S) \rangle$.

By contrast, Raman scattering peaks are dominated by incoherent signals. For these signals, the coherent emission is much smaller than total scattering intensity, i.e., $|\langle \mathbf{E}_S(\omega_S) \rangle|^2 \ll \langle |\mathbf{E}_S(\omega_S)|^2 \rangle$. To understand this, we show in Appendix B that, for a simplified model within the rotating wave approximation (RWA), the average electric field does not include a contribution at frequency $\omega_S = \Omega_{21}$. Instead, the signal is entirely incoherent. Note that, within Ehrenfest+R dynamics, this incoherence is introduced by applying the stochastic random phase operators in Eq. (17).

C. Resonant Raman cross section

We now turn our attention to the near-resonant regime, i.e., $\omega_I \approx \Omega_{20}$, and focus on Raman scattering. To compare against the KHD formula, we extract the scattering cross section from Ehrenfest+R dynamics by Eq. (32). In Fig. 2(a), we compare Ehrenfest+R dynamics with the KHD formula [Eq. (7)]. We demonstrate that Ehrenfest+R dynamics can quantitatively recover the enhancement of the Raman scattering cross section in the nearly resonant regime, while the standard Ehrenfest dynamics does not predict any enhancement. Furthermore, the linewidth obtained by the Ehrenfest+R approach agrees with the average lifetime for the KHD formula [Eq. (9)]. In Fig. 2(b), the difference between standard Ehrenfest and Ehrenfest+R results is plotted in logarithmic scale. The +R correction is necessary in order for semiclassical simulations to recover resonance Raman scattering.

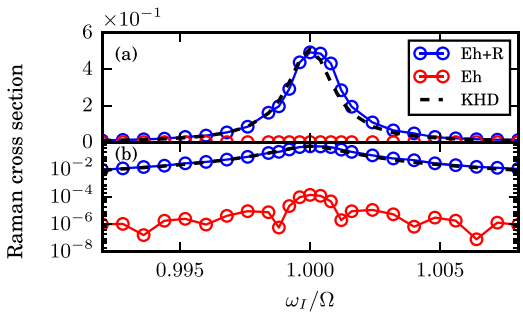


FIG. 2. The Raman scattering cross section as a function of incident frequency near resonance ($\omega_I/\Omega \approx 1$). Standard Ehrenfest dynamics are colored red, and Ehrenfest+R dynamics are colored blue. The KHD formula is plotted in dashed lines. The incoming field amplitude is $A_I/\sqrt{\hbar\Omega} = 6 \times 10^{-3}$. (a) is a linear plot, and (b) is a semi-log plot. Note that Ehrenfest+R dynamics match the KHD Raman signal, whereas Ehrenfest dynamics alone do not.

D. Field strength

Finally we focus on the intensity of resonance Raman scattering (i.e., $\omega_I = \Omega_{20}$) in response to various incident field amplitudes. Indeed, one might question whether or not the Raman signals as predicted by Ehrefenst+R dynamics scale correctly with respect to the EM field strength; indeed a devil's advocate might argue that these "Raman-like" features emerging from semiclassical dynamics are really non-linear features that arise from strong EM fields incident in the molecule. And yet, it is crucial to emphasize that Raman is a linear spectroscopy. From the KHD formula, the resonant scattering signal intensity in the weak field regime scales as $|\mathbf{E}_S| \sim A_I$ for all scattered frequencies ω_S,

$$\langle |\mathbf{E}_S(\omega_S)|^2 \rangle = A_I^2 \frac{\omega_S^2}{2\hbar^2 c^2} \frac{\mu^4}{\gamma^2}. \tag{36}$$

Here γ is given in Eq. (9). Furthermore, we note that, from Eq. (36), one can derive a simple relation for the ratio between the intensity of the Raman scattering ($\hbar\omega_S = \Omega_{21}$) and the intensity of the Rayleigh scattering ($\hbar\omega_S = \Omega_{20}$) given by

$$\frac{\langle |\mathbf{E}_S(\omega_S = \Omega_{21})|^2 \rangle}{\langle |\mathbf{E}_S(\omega_S = \Omega_{20})|^2 \rangle} = \left(\frac{\Omega_{21}}{\Omega_{20}} \right)^2. \tag{37}$$

Do Ehrenfest+R dynamics capture these scaling relationships? To answer these questions, in Fig. 3, we plot the Raman and Rayleigh scattering intensity signals as obtained from Ehrenfest+R dynamics as a function of A_I. We show conclusively that the Ehrenfest+R signals are linear with respect to A_I, in agreement with the KHD formula. This also shows that the ratio of the Raman and Rayleigh signals agrees with Eq. (37).

To contrast the coherent emission with the total scattering intensity, we also plot the coherent emission intensity ($|\langle E_S(\omega_S) \rangle|^2$) at the Raman and Rayleigh frequencies as a function of A_I. As we discussed above, the coherent emission of Raman scattering is approximately zero for all A_I. By contrast,

Published under license by AIP Publishing

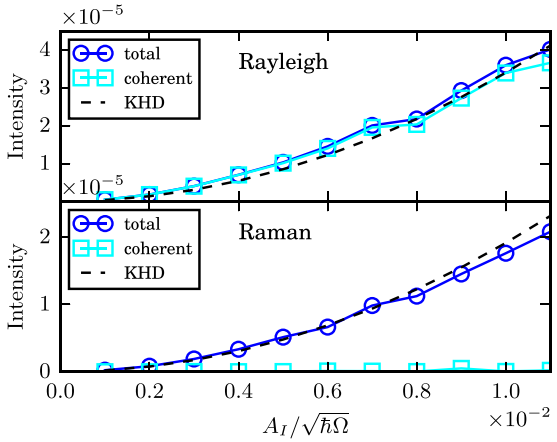


FIG. 3. The resonant scattering intensity as a function of incident CW amplitude A_I. The incident frequency is $\omega_I = \Omega_{20}$. The upper panel is the Rayleigh signal ($\omega_S = \Omega$), and the lower panel is the Raman signal ($\omega_S = \Omega_{21}$). For Ehrenfest+R dynamics, the blue circles represent the total intensity ($\langle|E_S(\omega_S)|^2\rangle$) and the cyan squares represent the coherent emission intensity ($|\langle E_S(\omega_S)\rangle|^2$). The black dashed line is the total intensity given by the KHD formula [Eq. (36)]. The value of the KHD intensity in the lower panel is exactly $(\Omega_{21}/\Omega_{20})^2 = (3/4)^2$ of the upper panel. Note that both KHD and Ehrenfest+R correctly capture the Raman and Rayleigh signals that are linear with respect to the incoming filed. Note also that the Raman signal is incoherent, whereas the Rayleigh signal is almost entirely coherent.

the signal at frequency $\omega_S = \omega_I = \Omega_{20}$ is almost exclusively a coherent Rayleigh scattering signal.

V. DISCUSSION AND CONCLUSIONS

In this work, we have generalized the Ehrenfest+R approach to treat a multi-level (more than two-level) system and we have demonstrated that such an approach recapitulates Raman scattering. In the context of a three-level system model, the proposed prescription of +R corrections can overcome the qualitative deficiencies of Ehrenfest dynamics and recover both resonant and off-resonant Raman scattering. In addition, a comparison with the quantum mechanical KHD formalism shows that Ehrenfest+R dynamics agrees quantitatively with resonant Raman scattering cross sections.

Given the promising results in this work, there are many further questions that need to be addressed. First, the proposed prescription is based on pairwise +R transitions with stochastic random phases for decoherence. If we take into account pure dephasing of the system, can this prescription of Ehrenfest+R dynamics produce the correct (and fully incoherent) fluorescence signals? More generally, have we found the optimal semiclassical approach for quantum electrodynamics with more than two electronic states? It will be very interesting to compare the present Ehrenfest+R approach with more standard nonadiabatic approaches, including partially linearized density matrix dynamics (PLDM),[39] Poisson-bracket mapping equation (PBME),[40] and symmetrical quantum-classical dynamics (SQC)[36,41,42] (which has shown great promise for spin-boson Hamiltonians). Second, the data in this work were generated for a three level system in one dimension only, assuming that the polarization density has a simple Gaussian profile. Does our prescription work for a system with arbitrary polarization density in three dimensions? Third, a three level system is usually not a proper model for off-resonant Raman scattering processes of molecular systems. Can the Ehrenfest+R approach be generalized to more than three level systems, ideally *ab initio* systems? Finally, the current setup includes one quantum subsystem only. How can we to treat the collective behavior of a set of molecular subsystems with strong electronic coupling? These questions will be investigated in the future.

ACKNOWLEDGMENTS

This material is based upon work supported by the U.S. Department of Energy, Office of Science, Office of Basic Energy Sciences under Award No. DE-SC0019397. The research of A.N. was supported by the Israel-U.S. Binational Science Foundation, the German Research Foundation (No. DFG TH 820/11-1), the U.S. National Science Foundation (Grant No. CHE1665291), and the University of Pennsylvania. M.S. was grateful to the financial support provided by the Air Force Office of Scientific Research under Grant No. FA9550-15-1-0189 and Binational Science Foundation under Grant No. 2014113.

APPENDIX A: SCATTERING CROSS SECTION IN A 1D SPACE

Here we derive the scattering cross section for a 1D system within the KHD formalism. Following Tannor's approach in Ref. 19, we make the rotating wave approximation (RWA) such that the electric dipole coupling can be written as $\hat{\mu}E_I e^{-i\omega_I t}/2$ for an incoming photon with amplitude E_I and frequency ω_I and $\hat{\mu}E_S e^{i\omega_S t}/2$ for an outgoing photon with amplitude E_S and frequency ω_S. (The amplitude E_S will be determined below.) Here $\hat{\mu}$ is the dipole operator of the electronic system. According to second order perturbation theory within the Schrödinger picture, the expression for the second order wavefunction is

$$|\psi^{(2)}(t)\rangle = -\frac{1}{4\hbar^2}\int_{-\infty}^{t} dt_2 \int_{-\infty}^{t_2} dt_1 e^{-\frac{i}{\hbar}\hat{H}_0(t-t_2)}\left(\hat{\mu}E_S e^{i\omega_S t_2}\right) \times e^{-\frac{i}{\hbar}\hat{H}_0(t_2-t_1)}\left(\hat{\mu}E_I e^{-i\omega_I t_1}\right)e^{-\frac{i}{\hbar}\hat{H}_0 t_1}|\psi_i\rangle, \quad \text{(A1)}$$

where the initial state of the system is $|\psi_i\rangle$. Here $\hat{H}_0$ is the unperturbed Hamiltonian of the electronic system and $\hat{\mu}$ is the transition dipole operator.[43]

Now we would like to express the number of outgoing photons scattered per unit time in terms of the change in the second order wavefunction. To do so, we evaluate the time derivative of the second-order wavefunction and insert a complete set of final states $|\psi_f\rangle$ to obtain

Published under license by AIP Publishing

$$\frac{d}{dt}\left\|\psi^{(2)}(t)\right\|^2 = \frac{2\pi E_S^2 E_I^2}{16\hbar^2}\sum_f \left|\alpha_{fi}(\omega_I)\right|^2 \delta(\omega_S - \Delta\omega), \tag{A2}$$

where the frequency-dependent polarizability is defined by

$$\alpha_{fi}(\omega_I) = \frac{i}{\hbar}\int_0^\infty d\tau \left\langle \psi_f \left| \hat{\mu} e^{-\frac{i}{\hbar}\hat{H}_0\tau} \hat{\mu} e^{i(\omega_I+\omega_i)\tau} \right| \psi_i \right\rangle. \tag{A3}$$

Here $\Delta\omega = \omega_I + \omega_i - \omega_f$, and $\hbar\omega_i$ and $\hbar\omega_f$ are the energy levels of the initial and final states of the system. If we now invoke the 1D density of states for photons ($\rho(\omega_S) = \frac{L}{\pi c}$), we can eliminate the delta function in Eq. (A2) and write

$$\frac{d}{dt}\left\|\psi^{(2)}(t)\right\|^2 = \frac{L}{8\hbar^2 c} E_S^2 E_I^2 \left|\alpha_{fi}(\omega_I)\right|^2. \tag{A4}$$

Finally, in order to express the scattering cross section in terms of photon frequencies, we must calculate the amplitude of the scattered EM field in Eq. (A4) in terms of other physical observables. To do so, we note the simple and general relationship between the electric field amplitude E and the number of photons N in a volume L,

$$\frac{\epsilon_0 E^2}{2} = \hbar\omega \frac{N}{L}. \tag{A5}$$

Here $\frac{N}{L}$ is the photon density for a 1D system. Note that Eq. (A5) is valid for both incoming and scattered photons. For incoming photons, the incident field intensity satisfies

$$E_I^2 = N_I \frac{2\hbar\omega_I}{\epsilon_0 L}. \tag{A6}$$

For scattered photons, assuming spontaneous emission, we must have $N_S = 1$ such that

$$E_S^2 = \frac{2\hbar\omega_S}{\epsilon_0 L}. \tag{A7}$$

With these relations, we rewrite Eq. (A4) as

$$\frac{d}{dt}\left\|\psi^{(2)}(t)\right\|^2 = \frac{\omega_I\omega_S}{2c\epsilon_0^2}\frac{N_I}{L}\left|\alpha_{fi}(\omega_I)\right|^2. \tag{A8}$$

Finally, we divide Eq. (A8) by the incident photon flux ($\frac{N_I c}{L}$) and obtain the Raman scattering cross section for a 1D system

$$\sigma_{fi}^{1D}(\omega_S, \omega_I) = \frac{\omega_I\omega_S}{2c^2\epsilon_0^2}\left|\alpha_{fi}(\omega_I)\right|^2. \tag{A9}$$

APPENDIX B: COHERENT EMISSION INTENSITY OF RAMAN SCATTERING

Here, we derive the coherent emission intensity of a three-level system within the rotating wave approximation (RWA). We let $|1_\omega\rangle$ be a state of the EM field with one photon of mode ω and denote the vacuum state as $|\{0\}\rangle$. The dressed state representation of the total wavefunction can be written as

$$|\psi(t)\rangle = \sum_{j=0,1,2} C_{j,0}(t)|j;\{0\}\rangle + \sum_{j=0,1,2} C_{j,\omega}(t)|j;\omega\rangle. \tag{B1}$$

Here the basis consists of $|j;\{0\}\rangle = |j\rangle|\{0\}\rangle$ and $|j;\omega\rangle = |j\rangle|1_\omega\rangle$ including up to a single photon per mode. For the incoming photon of mode ω_I, we choose the initial state to be

$$|\psi(0)\rangle = C_{0,0}|0;\{0\}\rangle + C_{0,\omega_I}|1;\omega_I\rangle, \tag{B2}$$

with $\left|C_{0,0}\right|^2 + \left|C_{0,\omega_I}\right|^2 = 0$. Here, we are approximating a weak coherent state as the sum of zero and one photon states only.

Now we assume that the incoming field is at resonance with states $|0\rangle$ and $|2\rangle$, i.e., $\hbar\omega_I = \varepsilon_2 - \varepsilon_0$. The Raman scattering frequency is $\hbar\omega_R = \varepsilon_2 - \varepsilon_1$, and the Rayleigh scattering frequency is $\hbar\omega_I$. Within the RWA, we consider the resonant states $|0;\omega_I\rangle$, $|1;\omega_R\rangle$, and $|2;\{0\}\rangle$ and write the RWA Hamiltonian as

$$\mathcal{H}_{RWA} = \begin{pmatrix} \varepsilon_0 + \hbar\omega_I & 0 & V_{02} \\ 0 & \varepsilon_1 + \hbar\omega_R & V_{12} \\ V_{02}^* & V_{12}^* & \varepsilon_2 \end{pmatrix}, \tag{B3}$$

where $V_{02} = -\mu_{02}A_I/\sqrt{2\epsilon_0}$ and $V_{12} = -\mu_{12}A_I/\sqrt{2\epsilon_0}$. In addition to the resonant states, the excited state $|2\rangle$ is coupled to the continuous manifolds, $\{|0;\omega\rangle, |1;\omega\rangle\}$. Therefore, the steady state solution can be expressed in terms of the resonant states and the initial vacuum state

$$\begin{aligned}\left|\overline{\psi_{RWA}}\right\rangle = {} & \overline{C_{0,0}}|0;\{0\}\rangle + \overline{C_{0,\omega_I}}|0;\omega_I\rangle + \overline{C_{1,\omega_R}}|1;\omega_R\rangle + \overline{C_{2,0}}|2;\{0\}\rangle \\ & + \sum_{\omega\neq\omega_I}\overline{C_{0,\omega}}|0;\omega\rangle + \sum_{\omega\neq\omega_I}\overline{C_{1,\omega}}|1;\omega\rangle.\end{aligned} \tag{B4}$$

Note that the vacuum state $|0;\{0\}\rangle$ is not coupled to the resonant states.

Finally, we can evaluate the coherent emission intensity using the expectation value of the electric field. For a 1D system, the electric field operator is given by

$$\hat{E}(x) = i\sum_k \mathcal{E}_k\left(\hat{a}_k e^{ikx} - \hat{a}_k^\dagger e^{-ikx}\right), \tag{B5}$$

with $\mathcal{E}_k = \sqrt{\frac{\hbar\omega_k}{2\epsilon_0 L}}$ in a space of volume L. Using the form of the steady state wavefunction, we can obtain the lowest order approximation of the expectation value of the electric field

$$\left\langle\hat{E}(x)\right\rangle = -2\mathcal{E}_k \mathrm{Im}\left(\overline{C_{0,0}}^* \overline{C_{0,\omega_I}} e^{i\omega_I x/c}\right). \tag{B6}$$

We note that there is not any contribution to the electric field at frequency ω_R since $\left\langle 1;\{0\}\middle|\overline{\psi_{RWA}}\right\rangle = 0$. Thus, the Fourier transform of the electric field vanishes at the Raman frequency,

$$|\langle E(\omega_R)\rangle| = 0. \tag{B7}$$

In other words, within the RWA, resonant Raman scattering does not yield coherent emission.

Therefore, we must conclude that, for a more general situation not far from RWA, all Raman scattering signals must be dominated by incoherent emission. As a sidenote, the arguments above also show that the Rayleigh peak should be

Published under license by AIP Publishing

coherent: the electric field in Eq. (B6) does not vanish at frequency $\omega_S = \omega_I$.

REFERENCES

[1]J. Gersten and A. Nitzan, J. Chem. Phys. **73**, 3023 (1980).
[2]D. A. Weitz, S. Garoff, J. I. Gersten, and A. Nitzan, J. Chem. Phys. **78**, 5324 (1983).
[3]K. A. Willets and R. P. Van Duyne, Annu. Rev. Phys. Chem. **58**, 267 (2007).
[4]P. L. Stiles, J. A. Dieringer, N. C. Shah, and R. P. Van Duyne, Annu. Rev. Anal. Chem. **1**, 601 (2008).
[5]S. M. Morton, D. W. Silverstein, and L. Jensen, Chem. Rev. **111**, 3962 (2011).
[6]P. Vasa and C. Lienau, ACS Photonics **5**, 2 (2018).
[7]X. Qian, X. Zhou, and S. Nie, J. Am. Chem. Soc. **130**, 14934 (2008).
[8]K. Qian, B. C. Sweeny, A. C. Johnston-Peck, W. Niu, J. O. Graham, J. S. DuChene, J. Qiu, Y.-C. Wang, M. H. Engelhard, D. Su, E. A. Stach, and W. D. Wei, J. Am. Chem. Soc. **136**, 9842 (2014).
[9]D. J. Masiello and G. C. Schatz, Phys. Rev. A **78**, 042505 (2008).
[10]N. Mirsaleh-Kohan, V. Iberi, P. D. Simmons, N. W. Bigelow, A. Vaschillo, M. M. Rowland, M. D. Best, S. J. Pennycook, D. J. Masiello, B. S. Guiton, and J. P. Camden, J. Phys. Chem. Lett. **3**, 2303 (2012).
[11]T. Hartman, C. S. Wondergem, N. Kumar, A. van den Berg, and B. M. Weckhuysen, J. Phys. Chem. Lett. **7**, 1570 (2016).
[12]E. M. Hiller and J. A. Cina, J. Chem. Phys. **105**, 3419 (1996).
[13]T. J. Smith and J. A. Cina, J. Chem. Phys. **104**, 1272 (1996).
[14]F. Le, D. W. Brandl, Y. A. Urzhumov, H. Wang, J. Kundu, N. J. Halas, J. Aizpurua, and P. Nordlander, ACS Nano **2**, 707 (2008).
[15]H. J. Butler, L. Ashton, B. Bird, G. Cinque, K. Curtis, J. Dorney, K. Esmonde-White, N. J. Fullwood, B. Gardner, P. L. Martin-Hirsch, M. J. Walsh, M. R. McAinsh, N. Stone, and F. L. Martin, Nat. Protoc. **11**, 664 (2016).
[16]H. A. Kramers and W. Heisenberg, Z. Phys. **31**, 681 (1925).
[17]P. A. M. Dirac and N. H. D. Bohr, Proc. R. Soc. London A **114**, 243 (1927).
[18]P. F. Bernath, *Spectra of Atoms and Molecules*, 3rd ed. (Oxford University Press, Oxford, New York, 2015).
[19]D. J. Tannor, *Introduction to Quantum Mechanics: A Time-Dependent Perspective* (University Science Books, Sausalito, California, 2006).
[20]A. C. Albrecht, J. Chem. Phys. **34**, 1476 (1961).
[21]J. Tang and A. C. Albrecht, *Raman Spectroscopy: Theory and Practice* (Springer, Boston, MA, 1970), pp. 33–68.
[22]D. A. Long, *The Raman Effect* (John Wiley & Sons, Ltd., Chichester, UK, 2002).
[23]S.-Y. Lee and E. J. Heller, J. Chem. Phys. **71**, 4777 (1979).
[24]E. J. Heller, Acc. Chem. Res. **14**, 368 (1981).
[25]E. J. Heller, R. Sundberg, and D. Tannor, J. Phys. Chem. **86**, 1822 (1982).
[26]D. J. Tannor and E. J. Heller, J. Chem. Phys. **77**, 202 (1982).
[27]J. Neugebauer and B. A. Hess, J. Chem. Phys. **120**, 11564 (2004).
[28]L. Jensen, J. Autschbach, and G. C. Schatz, J. Chem. Phys. **122**, 224115 (2005).
[29]L. Jensen, L. L. Zhao, J. Autschbach, and G. C. Schatz, J. Chem. Phys. **123**, 174110 (2005).
[30]D. Rappoport, S. Shim, and A. Aspuru-Guzik, J. Phys. Chem. Lett. **2**, 1254 (2011).
[31]M. Sukharev and A. Nitzan, J. Phys.: Condens. Matter **29**, 443003 (2017).
[32]Specifically, we refer to molecular systems adsorbed on plasmon-supporting metal surfaces. The interaction between molecular excitons and the local electromagnetic fields associated with a particular surface plasmonic mode of the metal modifies the exciton dynamics of the molecular subsystem. In the meantime, the molecular subsystem can have a significant effect on the plasmonic response of the metal, which is usually neglected in conventional treatments.
[33]P. W. Milonni, Phys. Rep. **25**, 1 (1976).
[34]A. Salam, *Molecular Quantum Electrodynamics: Long-Range Intermolecular Interactions* (John Wiley & Sons, Ltd., 2010).
[35]T. E. Li, A. Nitzan, M. Sukharev, T. Martinez, H.-T. Chen, and J. E. Subotnik, Phys. Rev. A **97**, 032105 (2018).
[36]W. H. Miller, J. Chem. Phys. **69**, 2188 (1978).
[37]H.-T. Chen, T. E. Li, M. Sukharev, A. Nitzan, and J. E. Subotnik, J. Chem. Phys. **150**, 044102 (2019); e-print arXiv:1806.04662.
[38]S. Mukamel, *Principles of Nonlinear Optics and Spectroscopy* (Oxford University Press, 1999).
[39]P. Huo and D. F. Coker, J. Chem. Phys. **137**, 22A535 (2012).
[40]H. Kim, A. Nassimi, and R. Kapral, J. Chem. Phys. **129**, 084102 (2008).
[41]S. J. Cotton and W. H. Miller, J. Phys. Chem. A **117**, 7190 (2013).
[42]S. J. Cotton and W. H. Miller, J. Chem. Phys. **139**, 234112 (2013).
[43]Formally, there is also another contribution to Eq. (A1) with the order of the operators $\hat{\mu}E_S e^{i\omega_S t}/2$ and $\hat{\mu}E_I e^{-i\omega_I t}/2$ switched. This term leads to another contribution to α_{fi} in Eq. (A3) which appears in the standard frequency-domain KHD formula.[20,25] However, this additional term corresponds to a relatively unlikely process whereby the system first emits an outgoing photon and then absorbs an incoming photon. For resonant Raman scattering, the contribution of this term can be ignored.

Published under license by AIP Publishing